Title

Deformation-based shape analysis of the hippocampus in the semantic variant of primary progressive aphasia and Alzheimer's disease

Permalink

https://escholarship.org/uc/item/9c4370k3

Authors

Chapleau, Marianne

Bedetti, Christophe

Devenyi, Gabriel A

et al.

Publication Date

2020

DOI

10.1016/j.nicl.2020.102305

Copyright Information

Peer reviewed

Deformation-based shape analysis of the hippocampus in the semantic variant of primary progressive aphasia and Alzheimer's disease

Marianne Chapleau[a,b], Christophe Bedetti[a,b], Gabriel A. Devenyi[c,d], Signy Sheldon[e], Howie J. Rosen[g], Bruce L. Miller[g], Maria Luisa Gorno-Tempini[g], Mallar M. Chakravarty[c,d,f], Simona M. Brambati[a,b,*]

[a] *Department of Psychology, University of Montreal, Quebec, Canada*
[b] *Research Center of l'Institut Universitaire de Gériatrie de Montréal, Quebec, Canada*
[c] *Computational Brain Anatomy Lab, Cerebral Imaging Center, Douglas Mental Health University Institute, Quebec, Canada*
[d] *Department of Psychiatry, McGill University, Quebec, Canada*
[e] *Department of Psychology, McGill University, Quebec, Canada*
[f] *Department of Biological and Biomedical Engineering, McGill University, Quebec, Canada*
[g] *Memory and Aging Center, University of California in San Francisco, CA, USA*

ARTICLE INFO

ABSTRACT

Background: Increasing evidence shows that the semantic variant of primary progressive aphasia (svPPA) is characterized by hippocampal atrophy. However, less is known about disease-related morphological hippocampal changes. The goal of the present study is to conduct a detailed characterization of the impact of svPPA on global hippocampus volume and morphology compared with control subjects and patients with Alzheimer's disease (AD).

Methods: We measured hippocampal volume and deformation-based shape differences in 22 patients with svPPA compared with 99 patients with AD and 92 controls. Multiple Automatically Generated Templates Brain Segmentation Algorithm (MAGeT-Brain) was used on MRI images obtained at the diagnostic visit.

Results: Comparable left and right hippocampal atrophy were observed in svPPA and AD. Deformation-based shape analysis showed a common pattern of morphological deformation in svPPA and AD compared with controls. More specifically, both svPPA and AD showed inward deformations in the dorsal surface of the hippocampus, from head to tail on the left side, and more limited to the anterior portion of the body in the right hemisphere. These results also pointed out that both diseases are characterized by a lateral displacement of the central part (body) of the hippocampus.

Discussion: Our study provides critical new evidence of hippocampal morphological changes in svPPA, similar to those found in AD. These findings highlight the importance of considering morphological hippocampal changes as part of the anatomical profile of patients with svPPA.

1. Introduction

The semantic variant of primary progressive aphasia (svPPA) is a neurodegenerative disease characterized by progressive deterioration of semantic memory (Gorno-Tempini et al., 2011; Hodges et al., 1992; Neary et al., 1998). In the early stages of the disease, patients with svPPA mainly manifest difficulties in confrontation naming, single word comprehension, and object knowledge in the context of relatively spared abilities in speech production (grammar and motor speech) and in word and sentence repetition (Gorno-Tempini et al., 2011; Neary et al., 1998). From an anatomical point of view, patients with svPPA

manifest bilateral atrophy of the anterior lateral temporal lobes, usually asymmetrical in the very early stages of the disease, and becoming bilateral as the disease progresses (Brambati et al., 2009, 2015; Davies et al., 2009; Galton et al., 2001; Mummery et al., 2000; Rohrer et al., 2008). However, growing evidence indicates that those suffering from svPPA could present significant hippocampal atrophy, even in early stages of the disease (Brambati et al., 2009; Chan et al., 2001; Chapleau et al., 2016; Davies et al., 2004; Desgranges et al., 2007; Galton et al., 2001; La Joie et al., 2014; Nestor et al., 2006).

An unresolved question is whether the hippocampal damage associated with svPPA presents similarities or dissimilarities with that of

---

Alzheimer's disease (AD). In fact, hippocampal atrophy is one of the main anatomical hallmarks of the limbic-predominant AD dementia (from now on referred to as AD) (Dubois et al., 2007; Frisoni et al., 2010) and is considered a neuroimaging biomarker for AD diagnosis and a possible target to determine the efficacy of disease-modifying treatments (Dubois et al., 2007). A detailed analysis of hippocampal damage in AD and its possible commonalities/differences with that of svPPA could provide important insight for disease identification and eventual pharmacotherapy.

The great majority of studies investigating the hippocampal degeneration in svPPA have used a volumetric approach (i.e., the segmentation of the hippocampus and the extraction of its global volume or the volume of its subparts), and they have provided varying results. Studies assessing the global volume of the hippocampus have provided critical evidence that patients with svPPA present decreased hippocampal volume compared with controls (Chapleau et al., 2016), yet direct comparisons of these volumes between AD and svPPA has yielded inconsistent results, with some studies reporting no differences between the groups (Nestor et al., 2006), some reported greater volume reductions in AD than svPPA (Davies et al., 2004; Lehmann et al., 2010), and other studies reported the opposite pattern (Barnes et al., 2006). Such inconsistent findings can be explained by these prior works relying on a single volumetric measure of the hippocampus to estimate atrophy. To our knowledge, the only study that compared the hippocampal subfields volumes in AD and svPPA found no differences between the two groups yet both patient populations had maximal volume decrease in the CA1 and subiculum subfields compared with controls (La Joie et al., 2013).

In this study, we compare hippocampal structural differences emerging in AD and svPPA using a sophisticated deformation-based shape analysis that provides volumetric as well as morphological information about the hippocampus. Morphological shape changes are represented by local areas of inward (contractions) or outward (expansions) displacements (Voineskos et al., 2015). Hippocampal shape analysis could be a useful tool for detecting signature sites of pathological changes in svPPA compared with controls and AD. Hippocampal shape changes have been consistently reported in studies comparing patients with AD to controls (Li et al., 2007; Scher et al., 2007; Wang et al., 2003, 2006). Globally, the results showed regional patterns of shape differences between AD and controls in regions approximately corresponding to the CA1 subfield (Li et al., 2007; Scher et al., 2007). However, the results varied across studies along the head-body-tail axis, where some authors found larger shape differences in the body than in the head (Scher et al., 2007), whereas others found larger shape differences in the head (Li et al., 2007). Additionally, whether shape changes in the hippocampus can differentiate between svPPA and AD has not been appropriately tested. To our knowledge, only one study has investigated hippocampal shape changes in AD and svPPA compared with controls within the same study (Lindberg et al., 2012). The authors have reported significant shape differences in the bilateral medial hippocampus in AD compared with controls, whereas this portion is relatively spared in svPPA (Lindberg et al., 2012). This study reported no direct comparison between svPPA and AD.

The goal of the present study is to conduct a detailed characterization of the impact of svPPA on hippocampal morphology compared with controls and patients with AD. To this aim, we performed a deformation-based shape analysis of the hippocampus on a sample of 22 patients with svPPA, 92 controls, and 99 patients with AD using the Multiple Automatically Generated Templates Brain Segmentation Algorithm (MAGeT-Brain; cobralab.ca/software/MAGeTBrain) (Pipitone et al., 2014). This approach is based on the multi-atlas automatic segmentation of the whole hippocampus (Voineskos et al., 2015) and has been successfully applied in population-based studies (Amaral et al., 2018; Pipitone et al., 2014). This method is suitable for the analysis of hippocampal morphology in a large sample.

2. Materials and methods

2.1. Participants

Data used in the preparation of this article were obtained from the UCSF Memory and Aging Center ADRC (P30 AG062422) database. We retrospectively identified all participants who received first-visit diagnoses of svPPA or AD or who were recruited as cognitively unimpaired controls. To be included in the study, participants must have had a usable high-resolution structural T1-weighted magnetic resonance image (MRI), obtained within 6 months of the diagnostic visit. The general exclusion criteria for all participants were as follows: native language other than English, left-handedness, developmental learning disabilities, history of a psychiatric disorder, history of traumatic brain injury, uncorrected hearing or vision problems, and motion or scanner artifacts in T1-weighted images. The patients with svPPA were diagnosed according to its currently accepted criteria (Gorno-Tempini et al., 2011). The diagnosis of AD was based on the criteria of the National Institute on Aging and the Alzheimer's Association workgroup (NIA-AA) (McKhann et al., 2011). As part of their assessment, all patients underwent a multidisciplinary evaluation including a neurological examination, neuropsychological assessment, caregiver interview, screening laboratory tests, and high-resolution structural T1-weighted magnetic resonance imaging (MRI). Global cognition and functional status were assessed using the Mini-Mental Status Examination (MMSE) (Folstein et al., 1975) and the Clinical Dementia Rating scale (CDR) (Morris, 1993) , respectively. Neuropsychological assessment included a previously described battery of standardized tests assessing memory, visuospatial abilities, and executive functions (Kramer et al., 2003). Patients with svPPA underwent a comprehensive speech and language evaluation for diagnostic purposes, including object naming, semantic and phonemic fluency, word and sentence comprehension, semantic association and repetition. (Gorno-Tempini et al., 2004)

We identified 36 patients with a clinical diagnosis of svPPA (19 women, 17 men), 106 patients with AD (60 women, 46 men), and 93 cognitively unimpaired controls (56 women, 37 men) recruited at the Memory and Aging Center UCSF. The three groups were matched for age (controls: mean age = 67.0, standard deviation (SD) = 3.9; svPPA: mean age = 66.5, SD = 7.2; AD: mean age = 66.9, SD = 10.4; H (2, 235) = 0.493, p = .781) and sex (χ2 (2, 235) = 0.643, p = .725).

The participants provided written informed consent, which was approved by the Internal Review Board of the University of California, San Francisco.

2.2. Image acquisition

The participants were scanned at the UCSF Neuroscience Imaging Center on a Siemens 3 Tesla Trio scanner using a body transmit coil and an 8-channel receive head coil. A T1-weighted 3D Magnetization Prepared Rapid Acquisition Gradient Echo (MPRAGE) was acquired with 160 sagittal slices, TE/TR/TI = 2.98/2300/900 ms, flip angle = 9°, isotropic voxel with size of 1 mm, field of view = 256 × 256 mm, and matrix = 256 × 256.

2.3. MRI data analysis

2.3.1. Preprocessing

The T1-weighted images were first preprocessed using minc-bpipe-library (https://github.com/CobraLab/minc-bpipe-library). This step ensured a standardization of images and included the following: bias field correction using N4ITK algorithm (Tustison et al., 2010), brain extraction using BEaST (Eskildsen et al., 2012), and field-of-view cropping to remove the neck. It provides standardized outputs in native space for further processing and in stereotaxic space for quality control. All images were closely observed for correct intensity homogeneity and brain extraction. None of the images were discarded due to quality control failure following this step.

2.3.2. Hippocampal segmentation

The well-validated Multiple Automatically Generated Templates (MAGeT-Brain; https://github.com/CobraLab/MAGeTbrain) (Chakravarty et al., 2013) pipeline was used to automatically segment the hippocampus (Pipitone et al., 2014).

MAGeT-Brain performs automatic hippocampal segmentation based on five high-resolution *in vivo* reference atlases of the hippocampus. These atlases were obtained from the manual segmentation of high-resolution images from 2 males and 3 females, as described in prior work (Pipitone et al., 2014). The five reference atlases were registered to a subset of 21 MRI images (7 from controls, 7 svPPA, 7 AD) selected from the 235 MRI images included in our study (i.e. MRI images from svPPA, AD and control subjects included in the study) using transformations estimated by linear and nonlinear image registration. This step allowed creating 105 segmentation labels (5 atlases × 21 images) representing the study-specific template library of hippocampal segmentation. The use of a study-specific template library approach allows overcoming possible hippocampal segmentation errors due to the fact that the neuroanatomy of the reference atlases (based on the images of 5 healthy subjects) may not be representative of the neuroanatomy of the subjects included in the study. Each image from the template library was then registered to all subject images (including the subset of 21 images that were used to create the template library). Thus, 105 hippocampal segmentations (one for each template included in the template library) were generated for each subject included in the study. A conclusive segmentation for each subject was determined by using the segmentation label that most often occurs at a specific location, using a majority voting (Amaral et al., 2018; Pipitone et al., 2014; Winterburn et al., 2013).

To choose the subset of participant images for the template library, a first step named "Best Templates for MAGeT" (https://github.com/CobraLab/documentation/wiki/Best-Templates-for-MAGeT : developed by Min Tae M. Park, MD.) was followed and required us to 1) run the first part of MAGeT-brain to label our 235 participants with the five manually segmented atlases, 2) perform quality control of each atlas to participant combinations (235 images × 5 atlases = 1175 images), and 3) choose the best-performing 21 participants (7 participants per group) over the five atlases as our template library.

The morphometric branch of MAGeT-Brain was used to produce surface objects of both hippocampi for each participant, providing displacement measurements on each vertex of the surfaces, [i.e., inward (contractions) and outward (expansions) deformations] (Chakravarty et al., 2015; Raznahan et al., 2014). MINC-bpipe-library and MAGeT-Brain pipelines were used on Niagara, a super-computing cluster from Compute Canada (Ponce et al., 2019).

Each participant's segmentation label underwent a detailed quality control (QC) inspection by the first co-author (rater: M.C.) to identify gross segmentation errors and artifacts. The QC of the resulting hippocampal segmentation was executed on all images following official MAGeT-Brain guidelines (https://github.com/CobraLab/documentation/wiki/MAGeT-Brain-Quality-Control-(QC)-Guide). Briefly, the QC consisted of visualizing each subject's brain image with its corresponding hippocampal segmentation label overlaid on the image and determining how accurately the label demarcates (segments) the underlying hippocampus. The QC was based on a three-point rating scale where « 1 » corresponded to a perfect segmentation, « 0.5. » corresponded to a slight over or under segmentation (a few voxels mislabeled) and « 0 » corresponded to an obvious failure. Images that received the « 0.5 » label were excluded if more than 4–5 voxels for 4 + slices were under/over segmented.

2.3.3. Statistical analysis

One-way analysis of variance (ANOVA) was used to verify if overall group differences were found for demographic characteristics, except for sex where chi-square test was used. Bonferroni correction was used for *post-hoc* comparisons. Analyses were two-tailed with the significance level set at p < .05 and were carried out with scipy 1.3.1 module on python 3.7.

RStudio (https://www.rstudio.com) and the standardized RMINC Toolkit (https://github.com/Mouse-Imaging-Centre/RMINC) were used on a standardized Virtual Machine (https://github.com/CobraLab/MINC-VM) to assess the deformation-based shape analysis between the three groups for both hippocampi. One-way ANOVA was conducted to determine whether there were statistically significant differences between the three groups. Since significant differences were observed in the ANOVA model, further *t*-tests were conducted to detect significant differences in the following comparisons: svPPA vs. controls, AD vs. controls and svPPA vs. AD. Whole hippocampal volumes (left and right), mean displacements values (to account for possible nonlinear shifts), age, sex and intracranial volumes (ICVs) were extracted and included in the model as nuisance variables. A false discovery rate (FDR) threshold of 5% was used to correct for multiple comparisons.

3. Results

3.1. Characteristics of the participants included in the study

One out of 93 control subjects, 7 out of 106 AD and 14 out of 36 svPPA patients failed the QC of the hippocampal segmentation. They were thus excluded from the analysis. Subjects excluded from the analysis, regardless of group belonging, were significantly older (p = .016). No differences were found for sex, CDR or MMSE.

A total of 22 svPPA patients, 92 controls and 99 AD patients were included in the analysis (Table 1). The analyzed sample remained matched by age (controls: mean age = 67.0, SD = 3.9; svPPA: mean age = 65.3, SD = 8.3; AD: mean age = 66.2, SD = 10.2; H (2, 213) = 2.07, p = .355) and sex (controls: 56F, 36 M, svPPA: 10F, 12 M, AD: 59F, 40 M; χ2 (2, 213) = 1.80, p = .406). Kruskal-Wallis test showed that the Clinical Dementia Rating (CDR) measure had a significant effect between groups (H(2, 213) = 144.1, p < .001). A post-hoc analysis using Dunn's test with Bonferroni correction showed that the two patient groups were matched in terms of CDR scores (p = .808) and that both groups significantly differed from controls (both p < .001). Similarly, the three groups displayed significant differences for the Mini-Mental State Examination (MMSE) (H(2, 155) = 101.7, p < .001). Both AD and svPPA patients presented lower scores than

Table 1

. Demographic characteristics of controls, AD patients, and svPPA patients.

	Controls (*n* = 92)	AD (*n* = 99)	svPPA (*n* = 22)	*p* value	Group comparison
Demographics					
Sex (n) F/M	56/36	59/40	10/12	0.406	Controls = AD = svPPA
Mean age (in years) (s.d.)	67.0 (3.9)	66.2 (10.2)	65.3 (8.3)	0.355	Controls = AD = svPPA
Global dementia status					
MMSE mean score (s.d.)	29.3 (0.9)	19.6 (6.3)	24.3 (4.1)	≤ 0.001	Controls > AD = svPPA
CDR mean score (s.d.)	0.0 (0.0)	0.8 (0.6)	0.6 (0.3)	≤ 0.001	Controls > AD = svPPA

Abbreviations: AD = Alzheimer's Disease; CDR = Clinical Dementia Rating; MMSE = Mini-Mental State Examination; s.d. = standard deviation; svPPA = semantic variant of primary progressive aphasia.

controls (p < .001), whereas AD and svPPA patients presented similar scores (p = .116). To characterize the pattern of gray matter atrophy in svPPA and AD patients included in the study, a voxel-based morphometry (VBM) analysis was conducted on MRI images. Anatomical images were analyzed using Statistical Parametric Mapping software (SPM12; http://www.fil.ion.ucl.ac.uk/spm/software/spm12) under MATLAB 2017 (http://www.mathworks.com). Image pre-processing followed standard procedures, including image segmentation, creation of a custom template using diffeomorphic anatomical registration and applying exponentiated lie algebra (DARTEL) approach (Ashburner, 2007), normalization of the GM tissue images to the MNI space, modulation to preserve the total amount of GM of original images, and smoothing (isotropic Gaussian Kernel of 6 mm FWHM). Statistical analysis was performed on smoothed modulated GM images. The images of the three groups (svPPA, AD and controls) were entered in an ANOVA statistical model. Age, sex and total intracranial volume were entered in the model as covariates. Statistical differences between svPPA and controls (pattern of GM atrophy in svPPA) and between AD and controls (pattern of GM atrophy in AD) were tested at a statistical threshold of p < 0.05, using family-wise error (FWE) correction. The results are reported in Fig. 1 and Supplementary Tables 1 and 2.

3.2. Characteristics of svPPA patients excluded from the study

The QC revealed that the automatic hippocampal segmentation failed in 22 out of 235 participants, who were consequently excluded from the study. The vast majority of excluded cases (14 out of 22) belonged to the svPPA group. A total of 14 out of 36 svPPA patients, representing 39% of our initial sample, were excluded from the study. This result raised questions about the underlying cause of pipeline inaccuracy in these patients. No differences were observed between the included and excluded svPPA patients concerning age, sex, CDR and MMSE score. We then investigated the contrast in the pattern of GM atrophy between svPPA participants for which the pipeline provided accurate hippocampal segmentation ('included svPPA', n = 22) and those who failed the quality check ('excluded svPPA', n = 14), using VBM. No differences were observed between the two subgroups at the pre-established threshold of p < 0.05, family-wise error (FWE) corrected, probably due to the small number of subjects included in the analysis. However, using a more permissive threshold of p < 0.001 uncorrected, we observed a cluster of significant results located in the anterior left hippocampus, indicating that excluded svPPA participants

had more atrophy in this region than included svPPA participants. The peak voxel of this cluster showed a trend towards significance using the pre-established corrected threshold (x = −33, y = −24, z = -14, T = 5.64, p = 0.0058, FWE-corrected). Since the segmentation of the hippocampus was not accurate in the excluded svPPA subgroup, we could not compare the global hippocampal volumes between the two.

3.3. Whole hippocampal volumes

In order to determine whether there was a statistical difference in the whole hippocampal volumes among the groups, two separate between-groups one-way ANCOVA models were performed for the left and right hippocampus, with group as a factor of interest and age, sex and total ICVs entered as nuisance variables. The between-groups ANCOVA yielded a statistically significant effect for both the left (controls: Mean = 2357 mm^3, SD = 257; svPPA: Mean = 2008 mm^3; SD = 316; AD: Mean = 2101 mm^3, SD = 432; F(2,210) = 17.8, p < .001) and the right hippocampus (controls: Mean = 2793 mm^3, SD = 342; svPPA: Mean = 2597 mm^3; SD = 562; AD: Mean = 2590 mm^3, SD = 480; F(2,210) = 5.45, p = .005). To further analyze the differences in the volume averages between the three groups, we conducted a Bonferroni *post-hoc* analysis. The results showed that both svPPA and AD groups showed significantly smaller left volumes compared to controls (p < .001), and these volumes were comparable to each other (p = .373). Regarding the right hippocampus, AD patients had significantly smaller volumes compared to controls (p = .006) and svPPA and AD had comparable volumes (p = 1.00). The residuals of the ANCOVA models for left and right hippocampus of controls, AD patients and svPPA patients are reported in Fig. 2.

3.4. Shape analysis

The results of the hippocampus deformation-based shape analysis are presented in Fig. 3. Significant vertex-wise shape differences were found when we compared the two patient groups to the controls group (svPPA vs. controls, AD vs. controls) and between each other (svPPA vs. AD), controlling for age, sex, intracranial volume, and mean displacement values. The comparison between svPPA and controls showed significant shape differences in svPPA bilaterally, but more severe in the left hippocampus. When svPPA patients were compared to controls, the analysis showed inward shape differences on the dorsal surface of
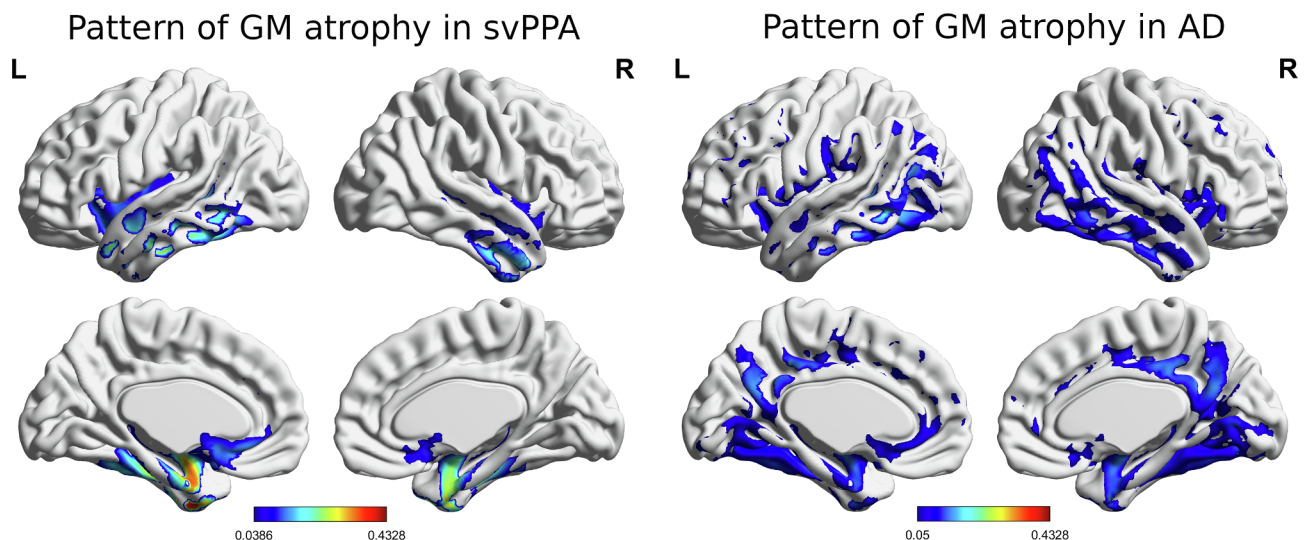

Fig. 1. Voxel-based morphometry results: pattern of gray matter atrophy in svPPA and AD displayed using BrainNet Viewer. The colors indicate the level of significance (p < 0.05, FWE-corrected, with blue being less significant than red). (For interpretation of the references to colour in this figure legend, the reader is referred to the web version of this article.)
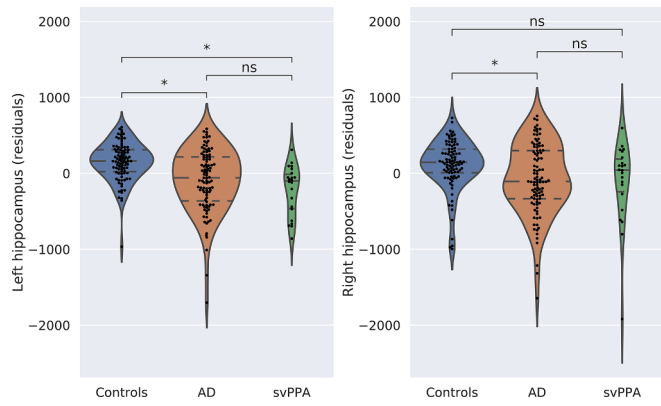
Fig. 2. Hippocampus volumetric differences. Residuals of the model with age, sex, and intracranial volume as covariates between controls, svPPA, and AD.

the hippocampus, from head to tail in the left hippocampus, and limited to the junction between the body and the head of the hippocampus in the right hippocampus. Moreover, in the left hippocampus, the results showed significant inward displacements in svPPA compared with controls in the medial portion of the hippocampus, and outward displacements in the lateral portion. These differences involved part of the head (see Fig. 3 left, superior view) and the body of the left hippocampus, relatively sparing the tail. A similar pattern of deformation changes was observed in the right hippocampus, although medial and superior inward deformations were mainly limited to the anterior portion of the body of the hippocampus. Moreover, the deformation pattern observed in the right hippocampus appeared less diffused compared with the pattern observed in the left one. The pattern observed in the contrast svPPA versus controls was generally similar to the one in the comparison between AD and controls. However, in AD, medial and superior inward deformations seemed to be more diffuse in both the left and the right hippocampus. In the left hippocampus, superior inward deformations also involved the most posterior portion of
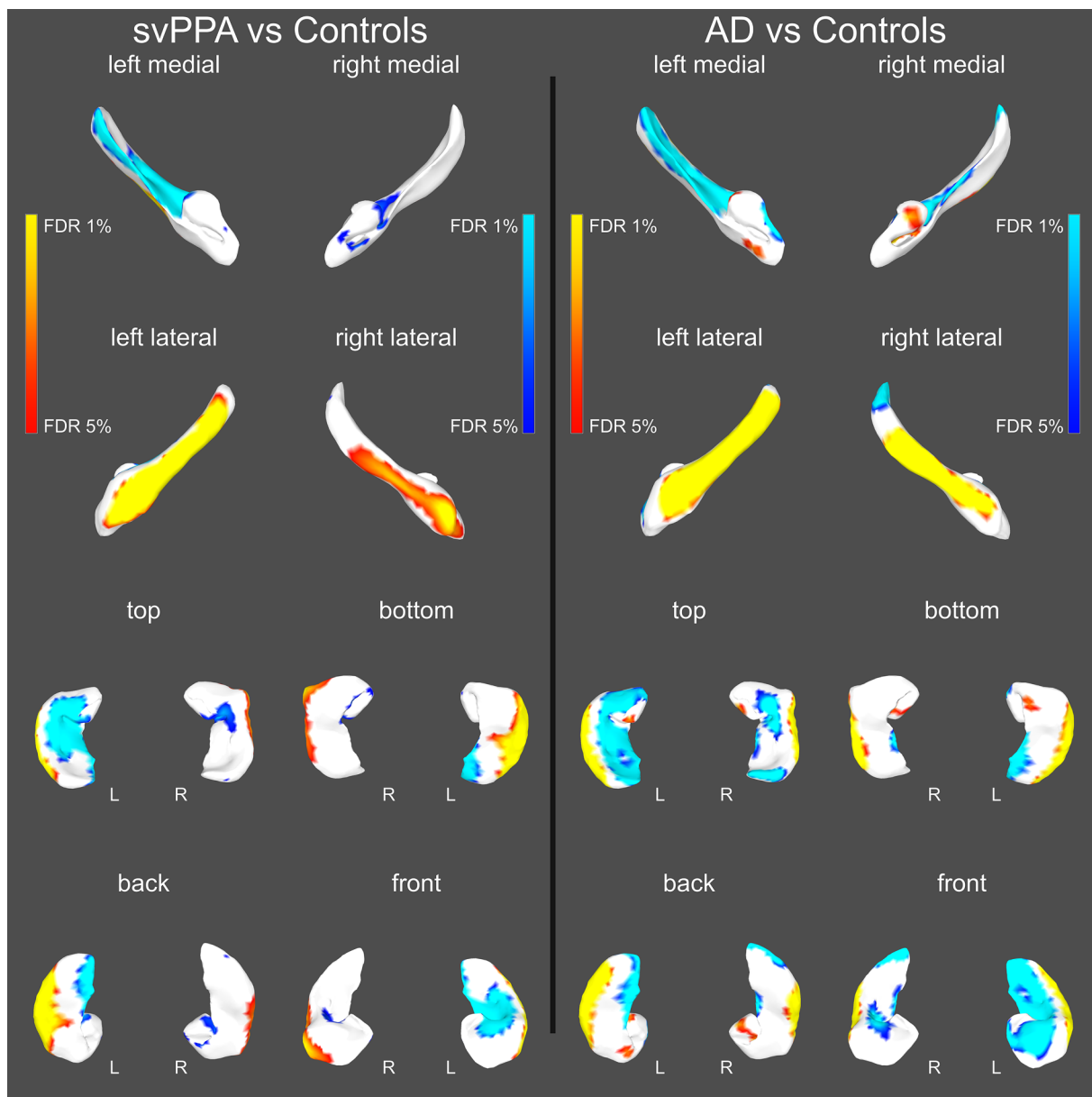

Fig. 3. Shape differences between svPPA vs. controls (left) and in AD vs. controls (right) controlling for age, sex, intracranial volume, and mean displacement values. Blue colors indicate regions with significant inward displacements in patients vs. controls; red regions indicate outward displacements. (For interpretation of the references to colour in this figure legend, the reader is referred to the web version of this article.)
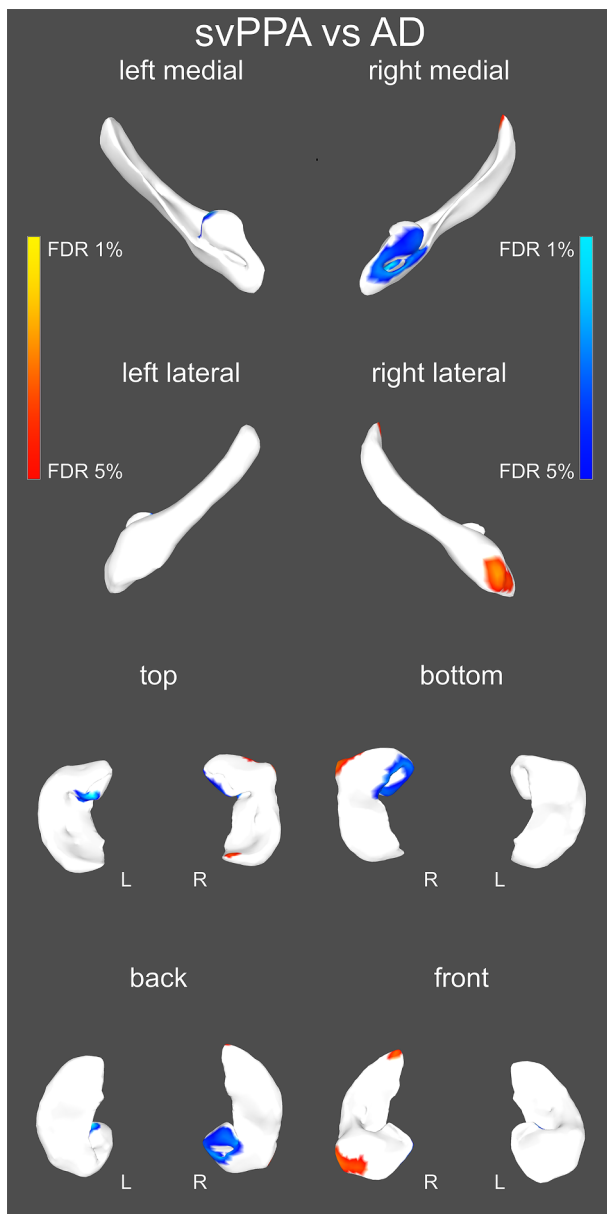
Fig. 4. Shape differences between svPPA and AD controlling for age, sex, intracranial volume, and mean displacement values. Blue colors indicate regions with significant inward displacements in svPPA vs. AD; red regions indicate outward displacements in svPPA vs. AD. (For interpretation of the references to colour in this figure legend, the reader is referred to the web version of this article.)

the hippocampus, whereas in the right hippocampus, it extended from the anterior part of the body of the hippocampus to the head (see Fig. 3 right, superior view). AD also presented outward differences compared with controls in the medial portion of the head of the hippocampus.

As observed in Fig. 4, svPPA, when compared with AD, showed inward shape differences in the medial and inferior portion of the head of the right hippocampus. This result probably reflects the fact that AD patients present outward deformations in this region (see the comparison AD vs. controls in Fig. 3 right) that are not significant in svPPA versus controls (see comparison svPPA vs. controls in Fig. 3 left). On the other hand, more severe outward deformations were observed in svPPA compared with AD in the lateral portion of the head of the right hippocampus.

4. Discussion

In this study we measured global volumetry and deformation-based shape differences of the hippocampus in 22 svPPA patients compared with 99 AD patients and 92 controls. Comparable left and right hippocampal global volumes were observed in svPPA and AD, controlling for the variance accounted for age, sex, and total intracranial volume. However, svPPA had significantly lower left hippocampal global volume than controls, but comparable right hippocampal volume. The shape analysis showed a common pattern of morphological deformation in svPPA and AD compared with controls. More specifically, both svPPA and AD showed inward deformations in the dorsal surface of the hippocampus, from head to tail in the left side, and more limited to the anterior portion of the body in the right hemisphere. This left–right asymmetry of deformation pattern seems to be more evident in svPPA than in AD. In addition, both svPPA and AD showed a pattern of outward shape deformation involving the lateral portion of the hippocampus and inward deformation mainly involving the medial and superior portion of the hippocampus. These results seem to indicate that both diseases are characterized by a lateral displacement of the central part (body) of the hippocampus. In the direct comparison between the two patient groups, svPPA patients showed larger outward deformation of the lateral part of the head of the right hippocampus, whereas AD patients showed larger inward deformation of the medial part of that same substructure, suggesting a possible displacement of the head toward the brain midline. No shape differences between svPPA and AD were observed in the left hippocampus. These data provide evidence of a global hippocampal volume reduction, and morphological shape changes that are part of the anatomical portrait of svPPA. Moreover, these disease-related hippocampal changes are similar to those observed in AD.

To the best of our knowledge, the present study is the first one to apply MAGeT-Brain automatic hippocampal segmentation to MRI images of patients with svPPA. Unfortunately, a total of 14 out of 36 svPPA patients, representing 39% of our initial sample, were excluded from the study because they failed the QC procedures. We have compared excluded and included svPPA participants in terms of demographic characteristics (age, sex), global cognition (MMSE) and functional status (CDR). The results revealed that the two subgroups were matched for all these variables. We then compared the pattern of GM atrophy between included and excluded svPPA participants using VBM in order to verify whether the excluded svPPA participants had more severe atrophy than the included ones. The results showed a trend towards significant more severe atrophy in the left hippocampus in the subgroup of excluded svPPA participants. The difference did not reach the threshold of significance, probably because of low statistical power due to small sample size (excluded svPPA, n = 14; included svPPA, n = 22). No differences were observed between the two subgroups besides a trend towards significant difference in the left hippocampus. One possible interpretation of this result is that the MAGeT-Brain pipeline faced more difficulties in terms of hippocampal segmentation in svPPA patients who presented more severe hippocampal atrophy. However, the reason why the majority of excluded cases belonged to the svPPA group, while only a minority (7 out of 106) belonged to the AD group also characterized by severe hippocampal atrophy (as revealed by the volumetric results), remains unclear. Further methodological studies aiming to improve the automatic segmentation in svPPA should be conducted in order to optimize the use of this approach in this patient population.

Bilateral hippocampal atrophy is generally accepted as a biomarker of AD (Jack et al., 2011; McKhann et al., 2011) and it has been proven to be a valuable tool for distinguishing AD from healthy controls (Laakso et al., 1998). Hippocampal atrophy occurs at early stages of the disease and atrophy pattern are observable throughout the brain as the disease progresses due to neuronal loss and neurofibrillary tangles (Braak & Braak, 1991). However, its specificity has been challenged by

the fact that hippocampal atrophy is common in other neurodegenerative diseases, such as svPPA. However, hippocampal volume loss was not consistently reported in svPPA. Several issues could have contributed to previous inconsistent results, including patient sample size, disease severity, and statistical models employed (e.g., inclusion of critical covariates such as age, sex and intracranial volumes in the model). Here we included a larger sample of svPPA patients than in most previous studies. The MRI images used in the present study were obtained at the timepoint of the diagnostic visit, suggesting that the patients were at relatively early stages of the disease. In addition, our svPPA sample showed relatively mild functional and global cognitive impairments, as assessed by the CDR and MMSE (CDR = 0.6 ± 0.4, MMSE = 24.3 ± 4.1). Nonetheless, we controlled for the variance explained by age, sex, and total intracranial volume in our group comparisons. Our results suggest that svPPA presents comparable volumes to AD in both the left and right hippocampus. It must be noted that while svPPA showed lower left hippocampal volume compared with controls in the left hemisphere, the results were less conclusive for the right hippocampus since no significant differences were observed either with controls or AD. This left asymmetrical atrophy pattern in svPPA is not surprising, given the fact that the anatomical presentation of the disease is usually asymmetrical, with the left hemisphere more damaged than the right, at least in the early stages of the disease (Brambati et al., 2009; Gorno-Tempini et al., 2004; Mummery et al., 2000; Rosen et al., 2002). It must be noted that our control group displayed bigger volume in the right compared to the left hippocampus. This asymmetry is consistent with the results of a previous meta-analysis (Pedraza et al., 2004). By pooling together the results of 82 studies (a total of 3,564 participants), the meta-analysis indicated that healthy adults show hippocampus asymmetry, with larger volumes in the right hemisphere (Pedraza et al., 2004). In conclusion, our results indicate global hippocampal atrophy in svPPA at relatively mild stages of the disease, challenging the diagnostic accuracy of this biomarker in distinguishing AD from svPPA.

In the present study, we used a surface-based analysis to provide complementary information to global volume analyses. In fact, surface analysis applied to the hippocampus allows mapping the vertex-based morphological properties of this structure, and it is a useful tool to detect possible displacements or deformations associated with specific diseases in clinical populations (Davatzikos & Bryan, 1996; Fischl et al., 1999, 2008; Tosun & Prince, 2008). Changes in hippocampal shape have been consistently reported in AD and its preclinical phases (Chetelat et al., 2008; Gerardin et al., 2009; Tepest et al., 2008; Wang et al., 2006). Our results showed inward deformation mainly involving the dorsal surface of the hippocampus in AD compared with controls, consistent with previous studies, mainly involving the left hemisphere. The dorsal hippocampus primarily performs the cognitive functions due to its connections with the medial and dorsolateral prefrontal cortex , as opposed to the ventral hippocampus, which is more focused on emotion processing and stress response due to its connections to the amygdala (Fanselow & Dong, 2010). Shape differences in the left hemisphere mainly involve regions of the dorsal CA1, but also CA2-3-4. Some previous studies have noted CA1 to be one of the most reliable markers to distinguish between early AD and subjects without dementia (Csernansky et al., 2000, 2005). However, hippocampal shape differences in AD are usually not limited to CA1 but also expand to CA2-3–4 (Frisoni et al., 2006; Wang et al., 2003). In the right hemisphere, differences in the shape of the dorsal surface were also reported but limited to the small surface between the head and the body of the hippocampus. Interestingly, in our study we generally found a similar pattern of shape deformations when we compared svPPA with controls. These results highlight how, at mild stages of the disease, svPPA pathology targets the hippocampus and affects its morphology in the dorsal surface. We also observed in both diseases a bilateral displacement of the body of the hippocampus. Critically, morphological changes, although more severe in the left hemisphere in svPPA, also involve the right side

in AD. These results seem to contradict the hypothesis that the bilateral hippocampus would be damaged in AD, and only the left one in svPPA (Chan et al., 2001; Galton et al., 2001). In fact, although the lateral anterior temporal lobes changes are usually asymmetrical, mainly affecting the left hemisphere, the hippocampal morphological changes seem to affect both the left and right hippocampus, even at mild stages of the disease. Shape differences in the left hippocampus, similar to those found in our study, were previously reported. However, in this study, shape differences in the right hippocampus did not survive False Discovery Rate (FDR) correction (Lindberg et al., 2012). This difference in the results can be due to the smaller sample size used in this study. It must be noted that the fact that we observed bilateral shape differences does not exclude the hypothesis that the primary site of pathology in svPPA is in the left hemisphere, and then spreading to the right one. In fact, the present study does not allow determining the evolution of morphological changes over time. Longitudinal studies in a large sample of patients are necessary to better determine the time course of the hippocampal morphological damage in svPPA.

In the direct comparison between the two patient groups, no differences were found in the left hippocampus. On the other hand, in the right hippocampus, svPPA patients showed larger inward deformation of the lateral part of the head of the right hippocampus, whereas AD patients showed larger inward deformation of the medial part of that same substructure. Previous studies have shown different roles of the lateral versus medial parts of the anterior hippocampus in relation to different cognitive functions. Previous work has showed that the lateral anterior hippocampus distinguishes past from future episodes, whereas the medial part of the anterior hippocampus would be more strongly activated when imagining specific past or future events rather than general events (Addis et al., 2011). Other studies have also found the medial anterior hippocampus to be engaged during functional magnetic resonance imaging (fMRI) tasks that require participants to vividly recall events from their past (Spreng et al., 2009). The medial anterior hippocampus would also be activated during imagination, recall, and perception of scenes (Zeidman & Maguire, 2016). These medial anterior hippocampus activations in various episodic/autobiographical mnemonic tasks are congruent with both our deformation-based results and the well-known cognitive deficiencies presented by amnestic AD patients (McKhann et al., 2011), as they have issues recalling events from their past. These cognitive deficits could thus be in part explained by the shape abnormalities found in the medial portion of the anterior hippocampus. However, this interpretation needs future investigation.

Our results raised the question why similar patterns of morphological damage in svPPA and AD result in different cognitive portraits in the two diseases, with the episodic memory mainly affected in AD and semantic memory in svPPA. Growing evidence supports the idea that cognitive deficits in neurodegenerative diseases would emerge from the widespread neural networks supporting specific cognitive functions rather than isolated brain regions (Seeley et al., 2009). Several studies have shown that different functional networks would be anchored to the hippocampus, with the anterior hippocampus being functionally more connected to the semantic network, and the posterior hippocampus to the episodic network (La Joie et al., 2014). Consistently, svPPA specifically affects the functional network anchored to the anterior hippocampus, and relatively spares the functional network anchored to the posterior hippocampus (Chapleau et al., 2019). However, this study did not analyze the network anchored to the lateral or medial portion of the head of the hippocampus. Future studies directly comparing both the structural and functional network of the hippocampus in the two populations, in association with their cognitive profiles, are necessary. These studies could potentially provide more specific biomarkers to differentiate the two diseases, and that could be used to follow the progression of the disease and the effect of new therapeutic trials. Moreover, studies using larger samples of svPPA patients would be necessary to draw global conclusions in terms of hippocampal neurodegeneration in this disease. In fact, we removed

several svPPA participants from our main analysis because MAGeT-Brain could not always segment thoroughly the hippocampus in these patients. An optimization of the pipeline could help conduct studies on larger samples of patients with svPPA or other atypical dementias.

In conclusion, our study provides critical new evidence that svPPA patients present hippocampal morphological changes similar to those found in AD at the time of the diagnostic visit, when the impact of the disease on global cognition and functional status is still relatively mild. These findings highlight the importance of considering morphological hippocampal changes as part of the anatomical profile of svPPA patients. These results challenge the role of hippocampal shape for differentiating these two diseases. Future studies are necessary to relate these findings to the cognitive profiles of these patients.

CRediT authorship contribution statement

Marianne Chapleau: Conceptualization, Formal analysis, Writing - original draft. **Christophe Bedetti:** Methodology, Software, Validation, Formal analysis, Writing - review & editing. **Gabriel A. Devenyi:** Methodology, Software, Validation, Formal analysis, Writing - review & editing. **Signy Sheldon:** Writing - review & editing. **Howie J. Rosen:** Resources, Funding acquisition, Project administration, Writing - review & editing. **Bruce L. Miller:** Resources, Funding acquisition, Project administration, Writing - review & editing. **Maria Luisa Gorno-Tempini:** Resources, Funding acquisition, Project administration, Writing - review & editing. **Mallar M. Chakravarty:** Methodology, Software, Validation, Formal analysis, Writing - review & editing. **Simona M. Brambati:** Conceptualization, Formal analysis, Writing - original draft, Supervision, Funding acquisition.

Acknowledgments

Appendix A. Supplementary data

Supplementary data to this article can be found online at https://doi.org/10.1016/j.nicl.2020.102305.

References

Addis, D.R., Cheng, T., Roberts, R.P., Schacter, D.L., 2011. Hippocampal contributions to the episodic simulation of specific and general future events. Hippocampus 21 (10), 1045–1052. https://doi.org/10.1002/hipo.20870.

Amaral, R.S.C., Park, M.T.M., Devenyi, G.A., Lynn, V., Pipitone, J., Winterburn, J., Chavez, S., Schira, M., Lobaugh, N.J., Voineskos, A.N., Pruessner, J.C., ChakravartyAlzheimer's Disease Neuroimaging, I., M.M., 2018. Manual segmentation of the fornix, fimbria, and alveus on high-resolution 3T MRI: Application via fully-automated mapping of the human memory circuit white and grey matter in healthy and pathological aging. Neuroimage 170, 132–150. https://doi.org/10.1016/j.neuroimage.2016.10.027.

Ashburner, J., 2007. A fast diffeomorphic image registration algorithm. NeuroImage 38 (1), 95–113. https://doi.org/10.1016/j.neuroimage.2007.07.007.

Barnes, J., Whitwell, J.L., Frost, C., Josephs, K.A., Rossor, M., Fox, N.C., 2006. Measurements of the amygdala and hippocampus in pathologically confirmed Alzheimer disease and frontotemporal lobar degeneration. Arch Neurol 63 (10), 1434–1439. https://doi.org/10.1001/archneur.63.10.1434.

Braak, H., Braak, E., 1991. Neuropathological stageing of Alzheimer-related changes. Acta Neuropathol 82 (4), 239–259.

Brambati, S.M., Amici, S., Racine, C.A., Neuhaus, J., Miller, Z., Ogar, J., Dronkers, N., Miller, B.L., Rosen, H., Gorno-Tempini, M.L., 2015. Longitudinal gray matter contraction in three variants of primary progressive aphasia: A tensor-based morphometry study. NeuroImag. Clinic. 8, 345–355. https://doi.org/10.1016/j.nicl.2015.01.011.

Brambati, S.M., Rankin, K.P., Narvid, J., Seeley, W.W., Dean, D., Rosen, H.J., Miller, B.L., Ashburner, J., Gorno-Tempini, M.L., 2009. Atrophy progression in semantic dementia with asymmetric temporal involvement: A tensor-based morphometry study. Neurobiol. Aging 30 (1), 103–111. https://doi.org/10.1016/j.neurobiolaging.2007.05.014.

Chakravarty, M.M., Rapoport, J.L., Giedd, J.N., Raznahan, A., Shaw, P., Collins, D.L., Lerch, J.P., Gogtay, N., 2015. Striatal shape abnormalities as novel neurodevelopmental endophenotypes in schizophrenia: A longitudinal study. Hum Brain Mapp 36 (4), 1458–1469. https://doi.org/10.1002/hbm.22715.

Chakravarty, M.M., Steadman, P., van Eede, M.C., Calcott, R.D., Gu, V., Shaw, P., Raznahan, A., Collins, D.L., Lerch, J.P., 2013. Performing label-fusion-based segmentation using multiple automatically generated templates. Hum Brain Mapp 34 (10), 2635–2654. https://doi.org/10.1002/hbm.22092.

Chan, D., Fox, N.C., Scahill, R.I., Crum, W.R., Whitwell, J.L., Leschziner, G., Rossor, A.M., Stevens, J.M., Cipolotti, L., Rossor, M.N., 2001. Patterns of temporal lobe atrophy in semantic dementia and Alzheimer's disease. Ann. Neurol. 49 (4), 433–442.

Chapleau, M., Aldebert, J., Montembeault, M., Brambati, S.M., 2016. Atrophy in Alzheimer's disease and semantic dementia: An ALE meta-analysis of voxel-based morphometry studies. J. Alzheimer's Dis. JAD 54 (3), 941–955. https://doi.org/10.3233/JAD-160382.

Chapleau, M, Montembeault, M, Boukadi, M, Bedetti, C, Laforce, R, Wilson, M, Brambati, SM, 2019. The role of the hippocampus in the semantic variant of primary progressive aphasia: A resting-state fcMRI study. Hippocampus 29 (11), 1127–1132. https://doi.org/10.1002/hipo.23156.

Chetelat, G., Fouquet, M., Kalpouzos, G., Denghien, I., De la Sayette, V., Viader, F., Mezenge, F., Landeau, B., Baron, J.C., Eustache, F., Desgranges, B., 2008. Three-dimensional surface mapping of hippocampal atrophy progression from MCI to AD and over normal aging as assessed using voxel-based morphometry. Neuropsychologia 46 (6), 1721–1731. https://doi.org/10.1016/j.neuropsychologia.2007.11.037.

Csernansky, J.G., Wang, L., Joshi, S., Miller, J.P., Gado, M., Kido, D., McKeel, D., Morris, J.C., Miller, M.I., 2000. Early DAT is distinguished from aging by high-dimensional mapping of the hippocampus Dementia of the Alzheimer type. Neurology 55 (11), 1636–1643. https://doi.org/10.1212/wnl.55.11.1636.

Csernansky, J.G., Wang, L., Swank, J., Miller, J.P., Gado, M., McKeel, D., Miller, M.I., Morris, J.C., 2005. Preclinical detection of Alzheimer's disease: Hippocampal shape and volume predict dementia onset in the elderly. Neuroimage 25 (3), 783–792. https://doi.org/10.1016/j.neuroimage.2004.12.036.

Davatzikos, C., Bryan, N., 1996. Using a deformable surface model to obtain a shape representation of the cortex. IEEE Trans. Med. Imaging 15 (6), 785–795. https://doi.org/10.1109/42.544496.

Davies, R.R., Graham, K.S., Xuereb, J.H., Williams, G.B., Hodges, J.R., 2004. The human perirhinal cortex and semantic memory. Eur. J. Neurosci. 20 (9), 2441–2446. https://doi.org/10.1111/j.1460-9568.2004.03710.x.

Davies, R.R., Halliday, G.M., Xuereb, J.H., Kril, J.J., Hodges, J.R., 2009. The neural basis of semantic memory: Evidence from semantic dementia. Neurobiol. Aging 30 (12), 2043–2052. https://doi.org/10.1016/j.neurobiolaging.2008.02.005.

Desgranges, B., Matuszewski, V., Piolino, P., Chetelat, G., Mezenge, F., Landeau, B., de la Sayette, V., Belliard, S., Eustache, F., 2007. Anatomical and functional alterations in semantic dementia: A voxel-based MRI and PET study. Neurobiol. Aging 28 (12), 1904–1913. https://doi.org/10.1016/j.neurobiolaging.2006.08.006.

Dubois, B., Feldman, H.H., Jacova, C., DeKosky, S.T., Barberger-Gateau, P., Cummings, J., Delacourte, A., Galasko, D., Gauthier, S., Jicha, G., Meguro, K., O'Brien, J., Pasquier, F., Robert, P., Rossor, M., Salloway, S., Stern, Y., Visser, P.J., Scheltens, P., 2007. Research criteria for the diagnosis of Alzheimer's disease: Revising the NINCDS–ADRDA criteria. Lancet Neurol. 6 (8), 734–746. https://doi.org/10.1016/S1474-4422(07)70178-3.

Eskildsen, S.F., Coupe, P., Fonov, V., Manjon, J.V., Leung, K.K., Guizard, N., Wassef, S.N., Ostergaard, L.R., CollinsAlzheimer's Disease Neuroimaging, I., D.L., 2012. BEaST: brain extraction based on nonlocal segmentation technique. Neuroimage 59 (3), 2362–2373. https://doi.org/10.1016/j.neuroimage.2011.09.012.

Fanselow, M.S., Dong, H.W., 2010. Are the dorsal and ventral hippocampus functionally distinct structures? Neuron 65 (1), 7–19. https://doi.org/10.1016/j.neuron.2009.11.031.

Fischl, B., Rajendran, N., Busa, E., Augustinack, J., Hinds, O., Yeo, B.T., Mohlberg, H., Amunts, K., Zilles, K., 2008. Cortical folding patterns and predicting cytoarchitecture. Cereb. Cortex 18 (8), 1973–1980. https://doi.org/10.1093/cercor/bhm225.

Fischl, B., Sereno, M.I., Dale, A.M., 1999. Cortical surface-based analysis. II: Inflation, flattening, and a surface-based coordinate system. Neuroimage 9 (2), 195–207. https://doi.org/10.1006/nimg.1998.0396.

Folstein, M.F., Folstein, S.E., McHugh, P.R., 1975. "Mini-mental state": A practical method for grading the cognitive state of patients for the clinician. J. Psychiatr. Res. 12 (3), 189–198. https://doi.org/10.1016/0022-3956(75)90026-6.

Frisoni, G.B., Fox, N.C., Jack, C.R., Scheltens, P., Thompson, P.M., 2010. The clinical use of structural MRI in Alzheimer disease. Nat Rev Neurol 6 (2), 67–77. https://doi.org/10.1038/nrneurol.2009.215.

Frisoni, G.B., Sabattoli, F., Lee, A.D., Dutton, R.A., Toga, A.W., Thompson, P.M., 2006. In vivo neuropathology of the hippocampal formation in AD: a radial mapping MR-based study. Neuroimage 32 (1), 104–110. https://doi.org/10.1016/j.neuroimage.2006.03.015.

Galton, C.J., Patterson, K., Graham, K., Lambon-Ralph, M.A., Williams, G., Antoun, N., Sahakian, B.J., Hodges, J.R., 2001. Differing patterns of temporal atrophy in Alzheimer's disease and semantic dementia. Neurology 57 (2), 216–225. https://doi.org/10.1212/wnl.57.2.216.

Gerardin, E., Chetelat, G., Chupin, M., Cuingnet, R., Desgranges, B., Kim, H.S., Niethammer, M., Dubois, B., Lehericy, S., Garnero, L., Eustache, F.,

ColliotAlzheimer's Disease Neuroimaging, I., O., 2009. Multidimensional classification of hippocampal shape features discriminates Alzheimer's disease and mild cognitive impairment from normal aging. Neuroimage 47 (4), 1476–1486. https://doi.org/10.1016/j.neuroimage.2009.05.036.

Gorno-Tempini, M.L., Dronkers, N.F., Rankin, K.P., Ogar, J.M., Phengrasamy, L., Rosen, H.J., Johnson, J.K., Weiner, M.W., Miller, B.L., 2004. Cognition and anatomy in three variants of primary progressive aphasia. Ann. Neurol. 55 (3), 335–346. https://doi.org/10.1002/ana.10825.

Gorno-Tempini, M.L., Hillis, A.E., Weintraub, S., Kertesz, A., Mendez, M., Cappa, S.F., Ogar, J.M., Rohrer, J.D., Black, S., Boeve, B.F., Manes, F., Dronkers, N.F., Vandenberghe, R., Rascovsky, K., Patterson, K., Miller, B.L., Knopman, D.S., Hodges, J.R., Mesulam, M.M., Grossman, M., 2011. Classification of primary progressive aphasia and its variants. Neurol. 76 (11), 1006–1014. https://doi.org/10.1212/WNL.0b013e31821103e6.

Hodges, J. R., Patterson, K., Oxbury, S., & Funnell, E. (1992). Semantic dementia. Progressive fluent aphasia with temporal lobe atrophy. Brain, 115 (Pt 6), 1783–806. https://doi.org/10.1093/brain/115.6.1783.

Jack, C.R., Barkhof, F., Bernstein, M.A., Cantillon, M., Cole, P.E., Decarli, C., Dubois, B., Duchesne, S., Fox, N.C., Frisoni, G.B., Hampel, H., Hill, D.L., Johnson, K., Mangin, J.F., Scheltens, P., Schwarz, A.J., Sperling, R., Suhy, J., Thompson, P.M., Foster, N.L., 2011. Steps to standardization and validation of hippocampal volumetry as a biomarker in clinical trials and diagnostic criterion for Alzheimer's disease. Alzheimers Dement 7 (4), 474–485.

Kramer, J.H., Jurik, J., Sha, S.J., Rankin, K.P., Rosen, H.J., Johnson, J.K., Miller, B.L., 2003. Distinctive neuropsychological patterns in frontotemporal dementia, semantic dementia, and Alzheimer disease. Cogn. Behav. Neurol. 16 (4), 211–218. https://doi.org/10.1097/00146965-200312000-00002.

Laakso, M.P., Soininen, H., Partanen, K., Lehtovirta, M., Hallikainen, M., Hanninen, T., ... Riekkinen, P.J., 1998. MRI of the hippocampus in Alzheimer's disease: Sensitivity, specificity, and analysis of the incorrectly classified subjects. Neurobiol. Aging 19 (1), 23–31.

La Joie, R., Landeau, B., Perrotin, A., Bejanin, A., Egret, S., Pelerin, A., Mezenge, F., Belliard, S., de La Sayette, V., Eustache, F., Desgranges, B., Chetelat, G., 2014. Intrinsic connectivity identifies the hippocampus as a main crossroad between Alzheimer's and semantic dementia-targeted networks. Neuron 81 (6), 1417–1428. https://doi.org/10.1016/j.neuron.2014.01.026.

La Joie, R., Perrotin, A., de La Sayette, V., Egret, S., Doeuvre, L., Belliard, S., Eustache, F., Desgranges, B., Chetelat, G., 2013. Hippocampal subfield volumetry in mild cognitive impairment, Alzheimer's disease and semantic dementia. Neuroimage Clin 3, 155–162. https://doi.org/10.1016/j.nicl.2013.08.007.

Lehmann, M., Douiri, A., Kim, L.G., Modat, M., Chan, D., Ourselin, S., Barnes, J., Fox, N.C., 2010. Atrophy patterns in Alzheimer's disease and semantic dementia: A comparison of FreeSurfer and manual volumetric measurements. Neuroimage 49 (3), 2264–2274. https://doi.org/10.1016/j.neuroimage.2009.10.056.

Li, S., Shi, F., Pu, F., Li, X., Jiang, T., Xie, S., Wang, Y., 2007. Hippocampal shape analysis of Alzheimer disease based on machine learning methods. AJNR Am J Neuroradiol 28 (7), 1339–1345. https://doi.org/10.3174/ajnr.A0620.

Lindberg, O., Walterfang, M., Looi, J.C., Malykhin, N., Ostberg, P., Zandbelt, B., Styner, M., Paniagua, B., Velakoulis, D., Orndahl, E., Wahlund, L.O., 2012. Hippocampal shape analysis in Alzheimer's disease and frontotemporal lobar degeneration subtypes. J. Alzheimers Dis. 30 (2), 355–365. https://doi.org/10.3233/JAD-2012-112210.

McKhann, G.M., Knopman, D.S., Chertkow, H., Hyman, B.T., Jack, C.R., Kawas, C.H., Klunk, W.E., Koroshetz, W.J., Manly, J.J., Mayeux, R., Mohs, R.C., Morris, J.C., Rossor, M.N., Scheltens, P., Carrillo, M.C., Thies, B., Weintraub, S., Phelps, C.H., 2011. The diagnosis of dementia due to Alzheimer's disease: Recommendations from the National Institute on Aging-Alzheimer's Association workgroups on diagnostic guidelines for Alzheimer's disease. Alzheimers Dement 7 (3), 263–269. https://doi.org/10.1016/j.jalz.2011.03.005.

Morris, J.C., 1993. The Clinical Dementia Rating (CDR): Current version and scoring rules. Neurology 43 (11), 2412–2414. https://doi.org/10.1212/wnl.43.11.2412-a.

Mummery, C.J., Patterson, K., Price, C.J., Ashburner, J., Frackowiak, R.S., Hodges, J.R., 2000. A voxel-based morphometry study of semantic dementia: Relationship between temporal lobe atrophy and semantic memory. Ann. Neurol. 47 (1), 36–45.

Neary, D., Snowden, J.S., Gustafson, L., Passant, U., Stuss, D., Black, S., Freedman, M., Kertesz, A., Robert, P.H., Albert, M., Boone, K., Miller, B.L., Cummings, J., Benson, D.F., 1998. Frontotemporal lobar degeneration: A consensus on clinical diagnostic criteria. Neurology 51 (6), 1546–1554. https://doi.org/10.1212/wnl.51.6.1546.

Nestor, P.J., Fryer, T.D., Hodges, J.R., 2006. Declarative memory impairments in Alzheimer's disease and semantic dementia. Neuroimage 30 (3), 1010–1020. https://doi.org/10.1016/j.neuroimage.2005.10.008.

Pedraza, O., Bowers, D., Gilmore, R., 2004. Asymmetry of the hippocampus and amygdala in MRI volumetric measurements of normal adults. J. Int. Neuropsychol. Soc. 10 (5), 664–678. https://doi.org/10.1017/S1355617704105080.

Pipitone, J., Park, M.T., Winterburn, J., Lett, T.A., Lerch, J.P., Pruessner, J.C., Lepage, M., Voineskos, A.N., ChakravartyAlzheimer's Disease Neuroimaging, I., M.M., 2014. Multi-atlas segmentation of the whole hippocampus and subfields using multiple automatically generated templates. Neuroimage 101, 494–512. https://doi.org/10.1016/j.neuroimage.2014.04.054.

Ponce, M., van Zon, R., Northrup, S., Gruner, D., Chen, J., Ertinaz, F., Fedoseev, A., Groer, L., Mao, F., Mundim, B. C., Nolta, M., Pinto, J., Saldarriaga, M., Slavnic, V., Spence, E., Yu, C.-H., & Peltier, W. R. (2019). Deploying a Top-100 Supercomputer for Large Parallel Workloads: The Niagara Supercomputer. Proceedings of the Practice and Experience in Advanced Research Computing on Rise of the Machines (Learning), 34:1–34:8. https://doi.org/10.1145/3332186.3332195.

Raznahan, A., Shaw, P.W., Lerch, J.P., Clasen, L.S., Greenstein, D., Berman, R., Pipitone, J., Chakravarty, M.M., Giedd, J.N., 2014. Longitudinal four-dimensional mapping of subcortical anatomy in human development. PNAS 111 (4), 1592–1597. https://doi.org/10.1073/pnas.1316911111.

Rohrer, J.D., McNaught, E., Foster, J., Clegg, S.L., Barnes, J., Omar, R., Warrington, E.K., Rossor, M.N., Warren, J.D., Fox, N.C., 2008. Tracking progression in frontotemporal lobar degeneration: Serial MRI in semantic dementia. Neurology 71 (18), 1445–1451. https://doi.org/10.1212/01.wnl.0000327889.13734.cd.

Rosen, H.J., Gorno-Tempini, M.L., Goldman, W.P., Perry, R.J., Schuff, N., Weiner, M., Feiwell, R., Kramer, J.H., Miller, B.L., 2002. Patterns of brain atrophy in frontotemporal dementia and semantic dementia. Neurology 58 (2), 198–208. https://doi.org/10.1212/wnl.58.2.198.

Scher, A.I., Xu, Y., Korf, E.S., White, L.R., Scheltens, P., Toga, A.W., Thompson, P.M., Hartley, S.W., Witter, M.P., Valentino, D.J., Launer, L.J., 2007. Hippocampal shape analysis in Alzheimer's disease: A population-based study. Neuroimage 36 (1), 8–18. https://doi.org/10.1016/j.neuroimage.2006.12.036.

Seeley, W.W., Crawford, R.K., Zhou, J., Miller, B.L., Greicius, M.D., 2009. Neurodegenerative diseases target large-scale human brain networks. Neuron 62 (1), 42–52. https://doi.org/10.1016/j.neuron.2009.03.024.

Spreng, R.N., Mar, R.A., Kim, A.S., 2009. The common neural basis of autobiographical memory, prospection, navigation, theory of mind, and the default mode: A quantitative meta-analysis. J. Cogn. Neurosci. 21 (3), 489–510. https://doi.org/10.1162/jocn.2008.21029.

Tepest, R., Wang, L., Csernansky, J.G., Neubert, P., Heun, R., Scheef, L., Jessen, F., 2008. Hippocampal surface analysis in subjective memory impairment, mild cognitive impairment and Alzheimer's dementia. Dement. Geriatr. Cogn Disord. 26 (4), 323–329. https://doi.org/10.1159/000161057.

Tosun, D., Prince, J.L., 2008. A geometry-driven optical flow warping for spatial normalization of cortical surfaces. IEEE Trans. Med. Imaging 27 (12), 1739–1753. https://doi.org/10.1109/TMI.2008.925080.

Tustison, N.J., Avants, B.B., Cook, P.A., Zheng, Y., Egan, A., Yushkevich, P.A., Gee, J.C., 2010. N4ITK: improved N3 bias correction. IEEE Trans. Med. Imaging 29 (6), 1310–1320. https://doi.org/10.1109/TMI.2010.2046908.

Voineskos, A.N., Winterburn, J.L., Felsky, D., Pipitone, J., Rajji, T.K., Mulsant, B.H., Chakravarty, M.M., 2015. Hippocampal (subfield) volume and shape in relation to cognitive performance across the adult lifespan: Hippocampal Volume, Shape, and Age-Related Cognitive Performance. Hum. Brain Mapp. 36 (8), 3020–3037. https://doi.org/10.1002/hbm.22825.

Wang, L., Miller, J.P., Gado, M.H., McKeel, D.W., Rothermich, M., Miller, M.I., Morris, J.C., Csernansky, J.G., 2006. Abnormalities of hippocampal surface structure in very mild dementia of the Alzheimer type. Neuroimage 30 (1), 52–60. https://doi.org/10.1016/j.neuroimage.2005.09.017.

Wang, L., Swank, J.S., Glick, I.E., Gado, M.H., Miller, M.I., Morris, J.C., Csernansky, J.G., 2003. Changes in hippocampal volume and shape across time distinguish dementia of the Alzheimer type from healthy aging. Neuroimage 20 (2), 667–682. https://doi.org/10.1016/S1053-8119(03)00361-6.

Winterburn, J.L., Pruessner, J.C., Chavez, S., Schira, M.M., Lobaugh, N.J., Voineskos, A.N., Chakravarty, M.M., 2013. A novel in vivo atlas of human hippocampal subfields using high-resolution 3T magnetic resonance imaging. NeuroImage 74, 254–265. https://doi.org/10.1016/j.neuroimage.2013.02.003.

Zeidman, P., Maguire, E.A., 2016. Anterior hippocampus: The anatomy of perception, imagination and episodic memory. Nat. Rev. Neurosci. 17 (3), 173–182. https://doi.org/10.1038/nrn.2015.24.